analytical chemistry

Article

pubs.acs.org/ac

# Label-Free Direct Visual Analysis of Hydrolytic Enzyme Activity Using Aqueous Two-Phase System Droplet Phase Transitions

David Lai,[†] John P. Frampton,[†] Michael Tsuei, Albert Kao, and Shuichi Takayama*

Department of Biomedical Engineering and Department of Macromolecular Science and Engineering, University of Michigan, Biointerfaces Institute, 2800 Plymouth Road, NCRC Building 10 A183, Ann Arbor, Michigan 48109, United States

Supporting Information

**ABSTRACT:** Dextran hydrolysis-mediated conversion of polyethylene glycol (PEG)-dextran (DEX) aqueous two-phase system droplets to a single phase was used to directly visualize Dextranase activity. DEX droplets were formed either by manual micropipetting or within a continuous PEG phase by computer controlled actuation of an orifice connecting rounded channels formed by backside diffused light lithography. The time required for the two-phase to one-phase transition was dependent on the Dextranase concentration, pH of the medium, and temperature. The apparent Michaelis constants for Dextranase were estimated based on previously reported catalytic constants, the binodal polymer concentration curves for PEG-DEX phase transition for each temperature, and pH condition. The combination of a microfluidic droplet system and phase transition observation provides a new method for label-free direct measurement of enzyme activity.

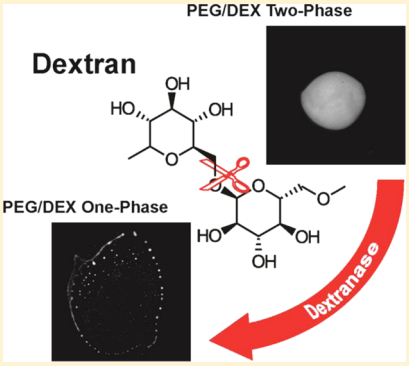


Assays for measuring the degradation of dextran (DEX) either require the use of specially prepared labeled polymers as surrogate substrates[1] or indirect measurement of degradation products, such as the amount of reducing sugar activity hydrolytically released from DEX.[2] Here, we describe a label-free direct visualization assay for the measurement of Dextranase activity that utilizes the observation of phase transitions of aqueous two-phase system (ATPS) droplets into one phase.

ATPSs are formed when two immiscible water-based solutions, usually composed of long-chain polymers, are mixed at concentrations above which it is thermodynamically favorable for the solutions to phase-separate into discrete regions.[3] This thermodynamic phenomenon is influenced by a variety of factors including pH, temperature, ionic content, solute/polymer concentration, and the molecular weight of the phase-separating constituents.[4] For aqueous polymer solutions of a given weight/weight concentration, solutions composed of larger molecular weight polymers phase-separate more readily because of the smaller entropic cost to demix the smaller number of distinct polymer chains. Thus, when an enzyme hydrolyzes polymers within an ATPS, phase separation becomes less favorable because either the weight/weight concentrations of the long-chain polymer decrease or the long-chain polymers become fragmented into shorter chains. While observations of hydrolysis-triggered phase transitions of macroscopic ATPSs requires large amounts of enzyme, reducing the volume of the polymer substrate phases using microfluidic principles makes such phase transition processes practical for the measurement of enzyme activity, thereby increasing throughput and reducing the amounts of reagents used.

The polyethylene glycol (PEG)-DEX ATPS is one of the most widely used ATPSs in laboratory science[5] and industry. The concentrations (typically expressed in terms of weight/weight) of PEG and DEX of certain molecular weights required for phase separation are described by binodal polymer concentration curves, as shown in Figure 1. A two-phase system will transition to a single phase if the concentrations of one or both polymers are decreased below the critical concentrations displayed by the binodal curve (Figure 1A). If one considers a phase diagram based on molar concentrations (a less common way to present ATPS phase diagrams), as the polymer molecular weight decreases the binodal curve shifts up. This means that even if the molar concentration of DEX and PEG remains constant, as the DEX molecular weight decreases due to degradation, the binodal curve shifts such that the same molar concentrations of polymers no longer produce phase separation. Dextranase degrades DEX to cause the DEX microdroplets formed in the PEG phase solutions to disappear due to phase transition (Figure 1A, right to left pointing horizontal arrow; Figure 1B, shifting of the binodal curve).

DEX hydrolysis by Dextranase is of significance to both the sugar/carbohydrate polymer industry and dental medicine. Here, we apply the thermodynamic principle of phase transition to measuring the enzymatic activity of Dextranase, an enzyme that hydrolyzes the $\alpha$-(1,6) glycosidic bonds of DEX to produce smaller oligosaccharides. We use well-plate and microfluidic droplet-based ATPS assays to demonstrate that the time it takes to transition a droplet-based PEG-DEX ATPS to a single

**Received:** February 17, 2014
**Accepted:** March 23, 2014
**Published:** March 23, 2014

   dx.doi.org/10.1021/ac500657k | *Anal. Chem.* 2014, 86, 4052−4057

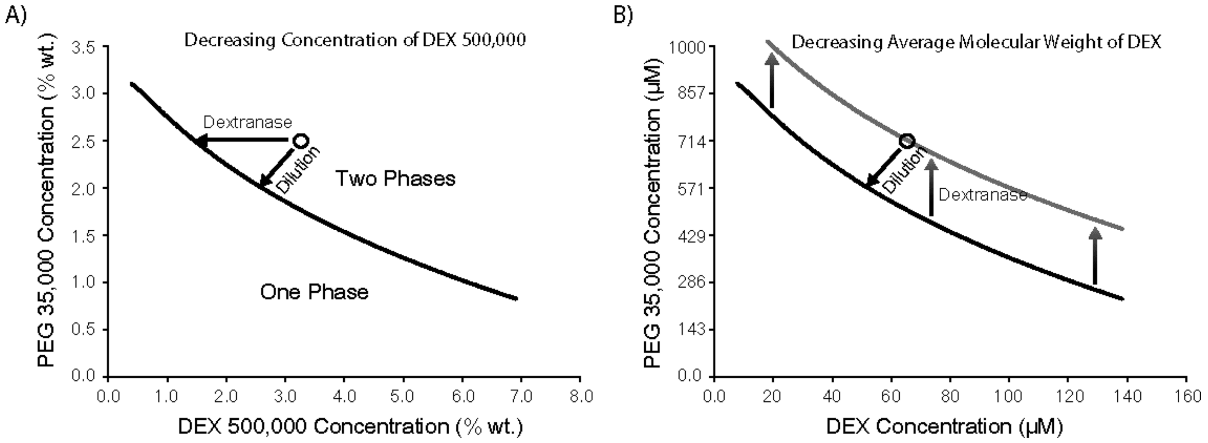


**Figure 1.** Binodal phase diagram for the PEG 35 000/DEX 500 000 system. (A) A two-phase system can be converted to a single phase either by dilution or by degradation of DEX by Dextranase. This graph focuses on the weight % concentration of DEX 500 000. (B) Another representation of how a two-phase system can be converted to a single phase either by dilution or by degration of DEX by Dextranase. This graph focuses on the molar concentration of long chain DEX of various molecular weights. As Dextranase digests DEX, the molar concentration remains the same for a significant time, but the average long chain DEX molecular weight decreases. As the molecular weight of DEX decreases, the molar concentration of DEX does not decrease, but the binodal curve shifts up because a higher concentration of PEG is required to form an ATPS with the same molar concentration of lower molecular weight DEX. The molar concentration point designated by the circle corresponds to 2.5% PEG 35 000/3.2% DEX 500 000.

phase depends on enzyme activity, as modulated by enzyme concentration, temperature, and pH of the ATPS solution. On the basis of our data, this process is not diffusion limited for the droplet sizes and enzyme concentrations we tested. The Michaelis constants for Dextranase activity are estimated for the various assay formats and enzyme conditions.

## EXPERIMENTAL SECTION

**Chemicals and Reagents.** DEX, average molecular weight 500 000, was purchased from Pharmacosmos (Denmark). Dextranase and PEG (average molecular weight 35 000) were both purchased from Sigma (MO). Microfluidic devices were fabricated from Sylgard 184 polydimethylsiloxane (PDMS) and curing agent, both purchased from Dow Chemical (MI). The master molds from which the microfluidic devices were replica-molded consisted of SU-8 from MicroChem (MA) patterned on glass coverslips from Fisher Scientific (MA).

**Aqueous Two-Phase Systems.** For the well-plate assays, a biphasic system composed of 2.5% PEG 35 000, 3.2% DEX T500, and PBS was formed. The equilibrated PEG and DEX phases were collected for Dextranase testing. For the microfluidic tests, ATPSs were formed from near-critical point DEX (~3.2% w/w) + 0.01% w/w FITC-DEX and PEG (2.5% w/w) in PBS. The ATPSs were equilibrated at room temperature and centrifuged at 600 rcf before use. For all Dextranase experiments, the pH was adjusted by addition of 1 N HCl to the PBS before incorporation of the polymers. Dextranase was added from a highly concentrated stock of 500 U/mL to achieve the appropriate concentration, where U is defined as 1 $\mu$mol of DEX degraded per minute in a pH 6.0 solution at 37 °C. Solutions were then stored on ice to prevent unwanted Dextranase activity.

**Dextranase Well-Plate Assays.** Images were acquired at specific time points (up to 210 min) to test the effects of Dextranase concentration (5, 2, 0.5, 0.2, 0.05, and 0.02 U/mL), pH (6.0 and 7.4) and temperature (25 and 37 °C) on DEX droplet degradation. After collection of the purified DEX and PEG phases, an appropriate amount of Dextranase was first added only to the DEX phase. After a defined preincubation period, 0.5 $\mu$L droplets of DEX/enzyme mixture were micropipetted into 48-well assay plates containing 200 $\mu$L of PEG in each well. The micropipetting step took no longer than 5 s. After 20 s, images of the DEX droplets were captured to definitively confirm the loss of the phase boundary and rule out the possibility of misidentifying a phase boundary due to differences in the refractive index of the solutions. The appearance of a stable interface between the DEX droplets and the bulk PEG phase indicated phase separation. Droplet dynamics, including spreading or contraction after droplet addition, were also noted. For the relatively few time points where phase transition could not be definitively confirmed, additional time points were collected and the average time between the first indication of interface disappearance (dramatic droplet expansion due to loss of interfacial tension and barely visible phase boundary) and definitive interface disappearance (clearly no phase boundary) was considered as the DEX degradation time. This type of experiment with preincubation of a DEX phase only solution followed by periodic addition of small aliquots of the degraded DEX phase solution into a PEG phase is important for obtaining insights into the role of diffusion (or lack thereof) versus reaction, since all of the DEX reactions take place without diffusion into PEG until the DEX droplets are added to PEG. The procedure, however, is tedious. Thus, to demonstrate improved time resolution with less hands-on activity from the experimenter, we also performed experiments where we dispensed DEX droplets containing Dextranase into the PEG solution and used time-lapse imaging every 2 s from 0 to 120 min to observe DEX droplet degradation continuously using single small droplets.

**Droplet Generating Device Fabrication.** Microfluidic devices were fabricated using backside diffused light lithography, as described previously.[6] Briefly, an SU-8-coated glass coverslip was exposed from the back (glass side) to UV illumination passing through a photomask. Rounded multilevel structures were developed in the photoresist using a discontinuous pattern on the photomask, such that light passing through the photoresist and the glass slide was scattered, exposing the SU-8 in the region corresponding to


dx.doi.org/10.1021/ac500657k | Anal. Chem. 2014, 86, 4052−4057

the discontinuity to less illumination. This diffuse light from both discontinuous ends joined to form a channel constriction (orifice) at the hydrodynamic focusing junction. The positive features from the photoresist were replica-molded using conventional soft lithography in PDMS to form elastomeric channels that were subsequently plasma-bonded to a PDMS membrane (100 $\mu$m thickness) fabricated by spin coating at 200 rpm for 240 s followed by 2000 rpm for 5 s. The channel geometries were designed to align with a Braille pin-array that was programmed to actuate the channel constriction to induce droplet formation, as described previously.[7]

**Microfluidic Droplet Formation.** The appropriate amount of Dextranase was added to the DEX solution, which was stored on ice to limit the Dextranase activity. This solution was loaded into a cold syringe and placed on a syringe pump. Ice packs were used to keep the syringe and tubing connected to the device cool. Using the flow focusing channel, a threading regime was produced by syringe pump-driven flow at 0.01 mL/h and 0.07 mL/h for the DEX and PEG phases, respectively. An actuating Braille pin was placed underneath the orifice in the center channel to control the flow of DEX at 0.8333 Hz. The Braille pin was controlled using a customized circuit-board connected to a computer through a universal serial bus (USB) with its own custom user interface. The entire process of loading the chilled DEX/Dextranase solution and aligning the device prior to droplet generation lasted no longer than 15 min. Droplet flow was arrested by collapsing the upstream and downstream channel regions using clamps. This produced a closed system that allowed time-lapse imaging of droplet dynamics in the presence of Dextranase. Droplets were imaged by fluorescence and brightfield microscopy (Nikon TS100, Tokyo, Japan), with images acquired every 30 s for the control and 0.02 U/mL Dextranase conditions and every 10 s for the 5 U/mL Dextranase condition. For microfluidic enzyme tests at temperatures above normal room temperature (~25 °C), the entire microscope room temperature was raised using climate control and further raised to 45 °C using a heat gun (Black & Decker, CT). The temperature was continually monitored using a thermometer and the room thermostat. Heating the entire room guaranteed a constant temperature for the microfluidic device and limited the effects of thermal gradients on the PEG-DEX ATPS.

**Calculation of Michaelis Constants.** The phase transition weight percentages of DEX for different DEX chain lengths at 2.5% PEG 35 000 for pH 7.4 at 25 °C were plotted and fitted with a power curve (Supplemental Figure 1 in the Supporting Information). The points in the graph were based on experimental phase diagrams and previously published phase diagrams for PEG 35 000 and DEX 500 000 (Supplemental Figure 2 in the Supporting Information), DEX 100 000,[8] DEX 40 000,[9] and DEX 10 000. The initial point of our ATPS corresponded to 2.5% PEG 35 000 and 3.2% DEX 500 000. As Dextranase digests the 500 000 g/mol DEX chain, the weight decreases proportionately to the fraction of the chain length digested. The expected molecular weight of DEX in the Dextranase assay at which phase transition occurs following Dextranase digestion is estimated to be 1.84% DEX 287 000 g/mol. The main products from digestion are glucose, isomaltose, isomaltotriose, and larger oligosaccharides.[10] We assumed that these products had insignificant contributions to phase formation.

The Michaelis–Menten kinetics allowed a comparison of the microwell assays and the microfluidic assay. For a given pH, the $K_{cat}$ of the assay is constant, while the $K_m$ changes. Varying the temperature from 37 to 25 °C changes the $K_{cat}$ according to the Arrhenius equation and also affects the $K_m$. The $K_m$ is described as

$$K_m = \frac{[S]K_{cat}[E]t}{[P]} - [S]$$

where [E] is the enzyme concentration, [S] is the concentration of long chain DEX, and [P] is the concentration of isomaltotriose. The rate constant at 37 °C is given by the manufacturer as 1.0 $\mu$mol/min/U. The activation energy, $E_a$, of the Arrhenius equation was determined from a previous study.[11] Thus, the $K_{cat}$ at 25 °C is 0.86 $\mu$mol/min/U. A Dextranase concentration of 2.0 U/mL was used for the well-plate assay calculations, and a concentration of 5.0 U/mL was used for the microfluidic assay calculations. Our experimental phase diagrams indicated that the phase transition weight percentage for DEX 500 000 varied only slightly with temperature and pH (from 1.466% to 1.543%). As such, identical values for [S] and [P] ($6.4 \times 10^{-8}$ and $2.7 \times 10^{-5}$ mol/mL, respectively) were used for each condition. [S] is based on the initial starting DEX concentration and [P] is calculated from the number of DEX chains ($6.4 \times 10^{-8}$) multiplied by the number of isomaltotriose units (504.44 g/mol) released per chain as it is digested from 500 000 g/mol to 287 000 g/mol (422). In this model, [S] (mol/mL) is approximated to be constant over time. This is not unreasonable, as the molar concentration of long-chain DEX is assumed not to change significantly within the time frame of our experiments. Instead, the molecular weight of the DEX decreases with enzymatic digestion. As isomaltotriose is released from each DEX chain, the DEX chain length will decrease, as will the weight percentage of DEX. Thus, the $K_m$ values for the various long-chain DEX polymers are expected to be similar. On the basis of these parameters, we calculated the Michaelis constants ($K_m$ values) as shown in Table 1.

**Table 1. Catalytic Data for the Various Dextranase Conditions and Assay Formats**

| enzyme condition | time (min) | $K_m$ (M) |
|---|---|---|
| Well-Plate Assay (Pre-Incubation) | | |
| pH 7.4, 25 °C | 100 | $3.4 \times 10^{-4}$ |
| pH 7.4, 37 °C | 35 | $1.0 \times 10^{-4}$ |
| pH 6.0, 25 °C | 22 | $2.4 \times 10^{-5}$ |
| pH 6.0, 37 °C | 15 | $7.1 \times 10^{-6}$ |
| Well-Plate Assay (Time-Lapse) | | |
| pH 7.4, 25 °C | 35 | $7.9 \times 10^{-5}$ |
| Microfluidic (Time-Lapse) | | |
| pH 7.4, 25 °C | 30[a] | $5.8 \times 10^{-5}$ |

[a]10 min was added to the time point shown in Figure 3b (20 min) to account for the additional time (including the time where temperature was kept low) that the DEX solution was exposed to Dextranase during microfluidic droplet generation preparation.

## RESULTS AND DISCUSSION

In this work, we maintained a constant PEG concentration, while degrading DEX by digesting it with Dextranase. This resulted in a decrease in the weight/weight concentration of the largest molecular weight DEX species (Figure 1A, right to left pointing horizontal arrow), while the molar concentration and total DEX-associated material mass of the system remained


dx.doi.org/10.1021/ac500657k | Anal. Chem. 2014, 86, 4052–4057

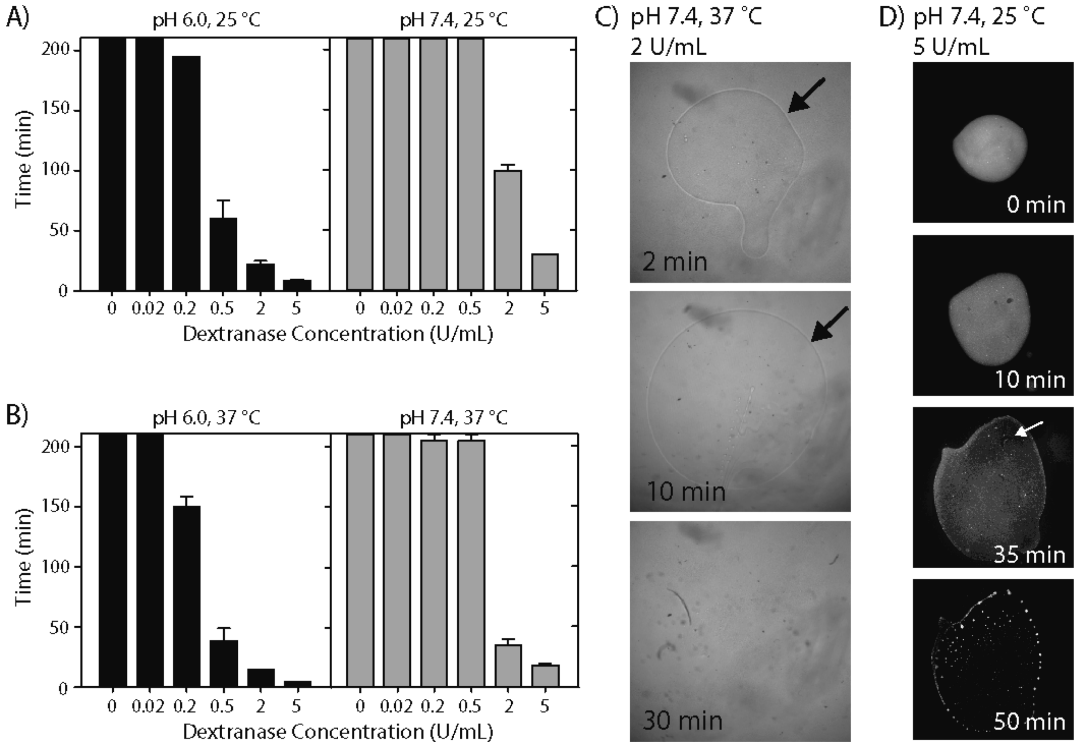


**Figure 2.** Two-phase to one-phase conversion occurs following Dextranase-mediated DEX degradation. (A,B) Dextranase activity can be assessed in a well-plate by recording the time at which DEX droplets preincubated with Dextranase no longer form phase boundaries with PEG. DEX droplet degradation times vary by pH, temperature, and Dextranase concentration. A maxium incubation time of 210 min was used for these assays. (C) Phase separation (or lack thereof) of DEX droplets preincubated with 2 U/mL Dextranase for 2, 10, and 30 min at pH 7.4, 37 °C as they are added into PEG. The black arrows indicate the phase boundary. (D) Phase separation of DEX droplets containing FITC-DEX and 5 U/mL Dextranase (without preincubation) in PEG, as recorded by fluorescence time-lapse imaging. The white arrow indicates the initial location of the void that indicated droplet degradation and the conversion of the ATPS to a single phase (see the Supplemental Video in the Supporting Information for additional data points). The 35 min time point was considered the transition point from two phases to one phase.

relatively constant. A two-phase to one-phase transition occurs when there is a decrease in weight/weight concentration of the original high molecular weight DEX (Figure 1A) or, if focusing on molar concentration of DEX of any molecular weight, when the molecular weights of the DEX decrease causing an upward shift of the binodal curve (Figure 1B). In contrast, diluting the solution would decrease the concentrations of both PEG and DEX and increase the overall volume of the solutions (Figure 1A, arrow toward the origin and Figure 1B).

We first tested the enzymatic hydrolysis-mediated aqueous two-phase system transition using DEX solution droplets of 0.5 $\mu$L formed by pipetting into a well-plate filled with PEG solution. Dextranase activity was modulated using three parameters: pH, temperature, and Dextranase concentration (Figure 2). Determination of two-phase to one-phase conversion was based on time-lapse experiments where aliquots of DEX phase solutions preincubated with Dextranase were added to a PEG phase at designated time intervals and the phase boundary at the DEX-PEG interface was observed immediately (~20 s) after addition to the PEG phase. At a few time points, only a portion of the boundary was visible. In those cases, the droplet system was determined to be in an intermediate state. In all cases, the intermediate state underwent two-phase to one-phase conversion by the time the next time point was observed. Increasing the pH from 6.0 to 7.4 increased the Dextranase-mediated time to DEX droplet degradation (i.e., the conversion from having the ability to maintain two-phases when added to the PEG phase to immediately becoming a one-phase upon addition) by ~3-fold (Figure 2A,B). Reducing the temperature from 37 to 25 °C also increased the time to DEX droplet degradation. Dextranase concentration was inversely proportional to time to DEX droplet degradation, displaying a nearly linear relationship; for example, when the Dextranase concentration was increased by 10-fold, the DEX droplet degradation time decreased by ~10-fold. These experiments where the DEX phase solutions were degraded first then added to the PEG phase solutions are important for confirming that the inability of the degraded DEX phase solution to form a two-phase system is not dependent on diffusion of the degraded molecules away from the DEX phase droplet. Rather, when a DEX droplet fails to form a two-phase system, it is mainly because the DEX polymers have been degraded sufficiently that phase separation cannot occur even though all of the original DEX polymer materials are still present (Figure 1). After dispensing the Dextranase-degraded DEX droplets into the PEG phase, the droplets generally spread out due to their low interfacial tension with the PEG phase, which makes the droplets flatter (Figure 2C). We also carried out a similar well-plate assay, in which DEX/FITC-DEX/Dextranase droplets were immediately placed in a PEG-filled well and observed by time-lapse imaging at 2 s intervals. The DEX droplet expanded over the course of imaging, before apparent voids began to appear in the droplet interior at ~35 min (Figure 2D). By 50 min, the droplet was completely consumed (see the Supplemental Video in the Supporting Information). We considered the 35 min time point to be the


dx.doi.org/10.1021/ac500657k | *Anal. Chem.* 2014, 86, 4052−4057

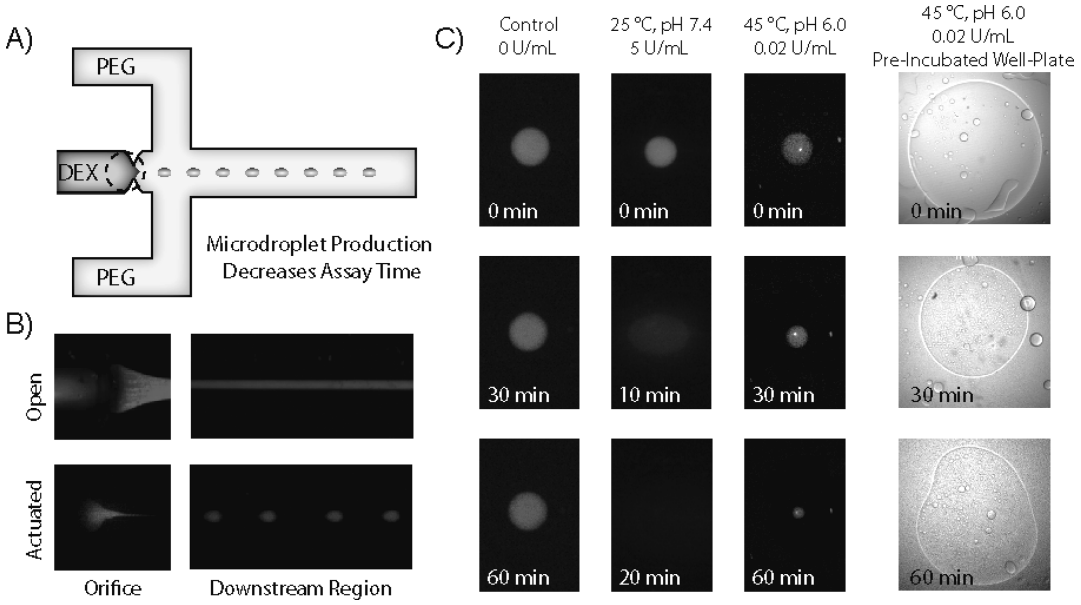


**Figure 3.** Operating principle of the droplet-generating device. (A) A central DEX inlet is flanked by two PEG inlets. The channel constriction is actuated by a computer controlled pin positioned at the black dashed circle. (B) Without actuation this constriction is open, resulting in the formation of a laminar stream of DEX in the center of the channel. Pin actuation at an appropriate frequency closes the constriction to produce droplets of DEX. The DEX phase was visualized using a FITC-DEX tracer. (C) Droplets generated microfluidically allow sensitive detection of enzyme activity. Droplet degradation was not observed when Dextranase was absent from the ATPS. (D) The preincubated well- plate assay produces comparable results for 0.02 U/mL Dextranase at pH 6.0, 45 °C.

point at which the two-phase to one-phase transition occurred in this assay.

This ATPS well-plate assay can be adapted for analysis of Dextranase activity in other aqueous solutions such as industrial/manufacturing batch solutions, cell culture media, and bacterial broth by simply observing the DEX-PEG phase transition. For more sensitive detection that may be necessary to assess small-scale bacterial Dextranase production, the assay detection limit can be lowered by decreasing the amount of DEX degradation required for two-phase to one-phase conversion. This can be achieved by using an ATPS composition that is closer to the binodal curve.

We next used a microfluidic device[12] to produce single- to subnanoliter DEX droplets to increase the throughput of the assay and demonstrate the potential for automated, chip-based analysis (Figure 3A–C). Without actuation from a computer-controlled pin, a laminar stream of DEX was formed in the microfluidic channel, enclosed by two streams of PEG. Upon actuation, flow was interrupted, resulting in formation of DEX droplets carrying FITC-DEX as a tracer material (Figure 3B). The FITC-DEX is not needed for purposes of measuring Dextranase activity but was included to help understand some of the dynamics of the degradation and droplet content release process, as will be explained below. We also monitored the droplets by brightfield microscopy.

In the absence of Dextranase, the droplets maintained their size, fluorescence intensity, and phase boundaries (Figure 3C, first column). The addition of Dextranase caused the degradation of the droplet emulsion into a single phase. At room temperature and a pH of 7.4, a high concentration of Dextranase (5 U/mL) was required to degrade the DEX droplets in a timely manner as these conditions are enzymatically not optimal (Figure 3C, second column). By adjusting the pH to 6.0 and increasing the temperature to 45 °C (the optimal enzymatic conditions for Dextranase), the DEX droplets could be degraded using much lower concentrations of Dextranase (0.02 U/mL) (Figure 3C, third column). We confirmed the time scale of droplet disappearance under this condition using the preincubated well-plate assays (Figure 3C, fourth column). These observations suggest various possibilities for designing rapid or gradual DEX-hydrolysis-triggered release of reagents from the DEX droplets.

To compare the different assay formats and enzyme degradation conditions, we calculated the Michaelis constants based on Michaelis–Menten kinetics and the binodal polymer concentration curves for the PEG-DEX ATPS (Table 1; binodal curves shown in Supplemental Figure 1 in the Supporting Information). The similarities in time to transitioning to one-phase between the DEX droplets preincubated with Dextranase before PEG addition and those that were incubated after addition to PEG, and the mechanistic explanation of Figure 1B suggest that the process of DEX/PEG two-phase to one-phase transition due to Dextranase degradation of DEX is not limited by diffusing away the degraded DEX. That is, DEX degradation products do not have to diffuse away for the phase transition to occur. Thus, our assay should be minimally influenced thermodynamically by changes in droplet scale. We do note, however, that there is slightly more ambiguity as to exactly when one considers a droplet to have transitioned to one phase (e.g., Figure 2D, 35 min) for larger droplets compared to smaller drops. As expected, the Michaelis constant decreased under conditions that were more favorable to enzymatic degradation of DEX (i.e., higher temperature and lower pH).

Our droplet dispersion technology has applications in the field of microfluidics,[13] where in the future it may be applied for microfluidic chemical reactions[14] or creating dynamic chemical gradients for studying cell signaling applications by compartmentalizing and releasing reagents or cell signaling factors. Since eukaryotic cells typically do not produce DEX and have


dx.doi.org/10.1021/ac500657k | Anal. Chem. 2014, 86, 4052–4057

few important glycosidic bonds hydrolyzed by Dextranase on their surface, the process may serve as a mild, cell culture-friendly, and localized controlled reagent-release mechanism. Dextranase is also of interest in clinical dentistry as it is secreted by oral bacteria that modify the formation of dental plaques and use the plaque constituents (including DEX) as a source of nutrients.[1] With the ability to detect Dextranase activities as low as 0.020 U/mL in less than 90 min (robust oral Dextranase-producing bacteria such as *P. Oralis* secrete extracellular Dextranase up to 0.490 U/mL[1]), it may be possible to analyze oral microbial flora using our system. Finally, highly sensitive Dextranase activity testing can be helpful in the sugar cane industry for early detection of costly and potentially destructive contamination, as well as for standardization of Dextranase enzymes used industrially to prevent DEX accumulation during sugar production.[15] While we focus on just the analysis of Dextranase activity, the concept of using aqueous two-phase system droplet transitions to directly visualize polymer hydrolyzing enzyme activity may be applicable to other biopolymer ATPSs as well.

## ■ ASSOCIATED CONTENT

### Supporting Information

Additional information as noted in text. This material is available free of charge via the Internet at http://pubs.acs.org.

## ■ AUTHOR INFORMATION


### Corresponding Author

*E-mail: takayama@umich.edu. Phone: 734-615-5539.


### Author Contributions

†David Lai and John P. Frampton contributed equally to this work.

The manuscript was written through contributions of all authors. All authors have given approval to the final version of the manuscript.

### Notes

The authors declare no competing financial interest.

## ■ ACKNOWLEDGMENTS

We thank the Coulter Foundation and NIH (Grant GM 096040) for funding.

## ■ REFERENCES


(1) Igarashi, T.; Yamamoto, A.; Goto, N. *Oral Microbiol. Immunol.* **1998**, *13* (6), 382−386.

(2) Kaster, A. G.; Brown, L. R. *Infect. Immun.* **1983**, *42* (2), 716−720.

(3) (a) Dobry, A.; Boyer-Kawenoki, F. *J. Polym. Sci.* **1947**, *2* (1), 90−100. (b) Albertsson, P. A. K., *Partition of Cell Particles and Macromolecules: Separation and Purification of Biomolecules, Cell Organelles, Membranes, and Cells in Aqueous Polymer Two-Phase Systems and Their Use in Biochemical Analysis and Biotechnology*, 3rd ed.; Wiley: New York, 1986; 346 pages.

(4) Albertsson, P. A. *Adv. Protein Chem.* **1970**, *24*, 309−341.

(5) (a) Tsukamoto, M.; Taira, S.; Yamamura, S.; Morita, Y.; Nagatani, N.; Takamura, Y.; Tamiya, E. *Analyst* **2009**, *134* (10), 1994−1998. (b) Yamada, M.; Kasim, V.; Nakashima, M.; Edahiro, J.; Seki, M. *Biotechnol. Bioeng.* **2004**, *88* (4), 489−494. (c) Soohoo, J. R.; Walker, G. M. *Biomed. Microdevices* **2009**, *11* (2), 323−329. (d) Tavana, H.; Jovic, A.; Mosadegh, B.; Lee, Q. Y.; Liu, X.; Luker, K. E.; Luker, G. D.; Weiss, S. J.; Takayama, S. *Nat. Mater.* **2009**, *8* (9), 736−741. (e) Tavana, H.; Mosadegh, B.; Takayama, S. *Adv. Mater.* **2010**, *22* (24), 2628−2631.

(6) (a) Futai, N.; Gu, W.; Takayama, S. *Adv. Mater.* **2004**, *16* (15), 1320−1323. (b) Lai, D.; Frampton, J. P.; Sriram, H.; Takayama, S. *Lab Chip* **2011**, *11* (20), 3551−3554.

(7) Gu, W.; Zhu, X.; Futai, N.; Cho, B. S.; Takayama, S. *Proc. Natl. Acad. Sci. U.S.A.* **2004**, *101* (45), 15861−15866.

(8) Boreyko, J. B.; Mruetusatorn, P.; Retterer, S. T.; Collier, C. P. *Lab Chip* **2013**, *13* (7), 1295−1301.

(9) Long, M. S. *Dynamic and asymmetric protein microcompartmentation in aqueous two-phase vehicles*. Doctoral Dissertation, Penn State University, State College, PA, 2005; accessed on February 15, 2014 at https://etda.libraries.psu.edu/paper/6801/.

(10) Fukumoto, J.; Tsuji, H.; Tsuru, D. *J. Biochem.* **1971**, *69*, 1113−1121.

(11) El-Tanash, A. B.; El-Baz, E.; Sherief, A. A. *Eur. Food Res. Technol.* **2011**, *233*, 735−742.

(12) Lai, D.; Frampton, J. P.; Hari, S. A.; Takayama, S. *Lab Chip* **2011**, *11* (20), 3551−3554.

(13) (a) Sugiura, S.; Nakajima, M.; Iwamoto, S.; Seki, M. *Langmuir* **2001**, *17* (18), 5562−5566. (b) Sugiura, S.; Nakajima, M.; Seki, M. *Langmuir* **2002**, *18* (15), 5708−5712. (c) Basu, A. S. *Lab Chip* **2013**, *13* (10), 1892−1901. (d) Zeng, S.; Pan, X.; Zhang, Q.; Lin, B.; Qin, J. *Anal. Chem.* **2011**, *83* (6), 2083−2089.

(14) (a) Trivedi, V.; Doshi, A.; Kurup, G. K.; Ereifej, E.; Vandevord, P. J.; Basu, A. S. *Lab Chip* **2010**, *10* (18), 2433−2442. (b) Schudel, B. R.; Choi, C. J.; Cunningham, B. T.; Kenis, P. J. A. *Lab Chip* **2009**, *9* (12), 1676−1680.

(15) Eggleston, G.; Monge, A. *Process Biochem.* **2005**, *40* (5), 1881−1894.